RESEARCH ARTICLE

Differential Distribution of microRNAs in Breast Cancer Grouped by Clinicopathological Subtypes

Jian-Yi Li, Shi Jia, Wen-Hai Zhang*, Yang Zhang, Ye Kang, Pi-Song Li

Abstract

Background: microRNAs (miRNAs) that regulate proliferation, invasion and metastasis are considered to be the principal molecular basis of tumor heterogeneity. Breast cancer is not a homogeneous tissue. Thus, it is very important to perform microarray-based miRNA screening of tumors at different sites. Methods: Breast tissue samples from the centers and edges of tumors of 30 patients were classified into 5 clinicopathological subtypes. In each group, 6 specimens were examined by microRNA array. All differential miRNAs were analyzed between the edges and centers of the tumors. Results: Seventeen kinds of miRNAs were heterogeneously distributed in the tumors from different clinicopathological subtypes that included 1 kind of miRNA in Luminal A and Luminal B Her2+ subtypes, 4 kinds in Luminal A and Her2 overexpression subtypes, 6 kinds in Luminal B Ki67+ and Luminal B Her2+ subtypes, 2 kinds between Luminal B Ki67+ and triple-negative breast cancer (TNBC) subtypes, 2 kinds between Luminal B Her2+ and TNBC subtypes, and 2 kinds between Luminal B Ki67+, Luminal B Her2+, and TNBC subtypes. Twenty kinds of miRNAs were homogenously distributed in the tumors from different clinicopathological subtypes that included 6 kinds of miRNAs in Luminal B Ki67+ and Luminal B Her2+ subtypes, 1 kind in Luminal B Ki67+ and Her2 overexpression subtypes, 10 kinds between Luminal B Ki67+ and TNBC subtypes, 2 kinds in Luminal B Her2+ and TNBC subtypes, and 1 kind between Luminal B Ki67+, Luminal B Her2+, and TNBC subtypes. Conclusions: A total of 37 miRNAs were significantly distributed in tumors from the centers to edges, and in all clinicopathological subtypes.

Keywords: microRNA - breast cancer - clinicopathological subtype - heterogeneity

Asian Pacific J Cancer Prev, **14 (5)**, 3197-3203

Introduction

The ambitious Human Genome Project did not lead to the elimination of cancer, cardiovascular or cerebrovascular diseases, as was originally expected; rather, it accelerated the birth of genomics, proteomics, and bioinformatics (Kreiner et al., 2005; Juan et al., 2007). MicroRNAs (miRNAs) are a class of endogenous, small, non-coding RNAs that control gene expression by interacting with target mRNAs, resulting in either mRNA degradation or translational repression (Pritchard et al., 2012). There is increasing evidence that miRNAs play important roles in cancer progression (Caporali et al., 2011). Since 2005, many studies have reported the discovery of novel miRNAs using microrray validation (Iorio et al., 2005). Microarray screening is commonly used to evaluate differentially expressed miRNAs between tumor and normal tissue in studies attempting to determine the relationship between miRNA dysregulation and human disease (Cheng et al., 2009). Optimal results are obtained from homogenous samples; however, solid tumors are not homogeneous. One of their main characteristics is heterogeneous microvessel distribution with significant hypoxia occurring in regions of decreased blood flow (Balsat et al., 2011). The distribution of miRNAs in breast tumors might be an important factor in breast cancer angiogenesis, invasion and metastasis, and as such, is worth examining in some detail. In this study, we classified tumors according to their clinicopathological subtypes based on the St. Gallen Breast Cancer Treatment Consensus 2011 (Goldhirsch et al., 2011). MiRNA Arrays were performed in the centers and edges of tumors from each clinicopathological subtype. Our data showed that many types of miRNAs were differentially distributed in the breast tumors. These results might further our understanding of the heterogeneity of miRNA expression in breast cancer.

Materials and Methods

Patients and groups

Thirty human breast tumor samples were obtained by open surgical resection from patients, who were treated at Shengjing Hospital of China Medical University

*Department of Breast Surgery, Shengjing Hospital of China Medical University, Shenyang, Liaoning Province, China *For correspondence: sjbreast@sina.com, zhangwh@sj-hospital.org*

Table 1. Entry Criteria and Patient Parameters

Parameters		Luminal A (n=6)	Luminal B Ki67+ (n=6)	Luminal B Her2+ (n=6)	Her2 OE (n=6)	TNBC (n=6)
Age(years)	MEAN	48.50±9.46	50.17±7.78	45.50±9.20	43.17±9.66	42.83±8.98
	Range	38~66	39~59	36~57	29~53	28~53
Menopause	Yes	1	3	2	1	2
	No	5	3	4	5	4
Quadrant	Areolar	1	0	0	1	0
	Outer upper	4	3	4	2	3
	Outer lower	0	2	1	0	1
	Inner lower	0	0	0	2	1
	Inner upper	1	1	1	1	1
Operation	Mastectomy	5	5	3	5	4
	Tumorectomy	1	1	3	1	2
Diameter (2cm≤D≤3cm)		2.57±0.34	2.59±0.31	2.45±0.34	2.32±0.33	2.53±0.24
Histological Grade	I	6	6	0	0	0
	II	0	0	3	0	0
	III	0	0	3	6	6
Node Metastasis	No	6	6	0	0	0
	Yes	0	0	6	6	6
Cancer Thrombosis	No	6	6	0	0	0
	Yes	0	0	6	6	6
ER	Negative	0	0	0	6	6
	Positive	6	6	6	0	0
PR	Negative	0	0	4	6	6
	Positive	6	6	2	0	0
Her2	Negative	6	6	0	0	6
	Positive	0	0	6	6	0
Ki67	Negative	6	0	3	0	0
	Positive	0	6	3	6	6
P53	Negative	6	6	2	0	0
	Positive	0	0	4	6	6
Clinical Stage	IIA	6	6	0	0	0
	IIB	0	0	6	6	6

Description: Inclusion criteria included invasive ductal carcinoma, tumor diameter between 2 and 3 cm, no family history of neo-adjuvant therapy and radiotherapy, no family history of other cancers, and no accessory breast cancer

(SJHCMU) between 2005 and 2012. Inclusion criteria were: invasive ductal carcinoma (IDC), tumor diameter between 2 and 3 cm, clinical stage II, no history of neo-adjuvant therapy and radiotherapy, no family history of breast cancer and other cancers, and no accessory breast cancer. Pathological tumor stage was assessed according to the criteria described in the 6th edition of the American Joint Committee on Cancer (AJCC) staging manual. The tumors were classified into histological grades I–III according to the Nottingham combined histological grading system. Of those patients, six met the requirements and entered the Luminal A group; the patient characteristics in this group were: no lymph node metastases, histological grade I, human epidermal growth factor receptor 2 (Her2)-negative, vascular cancer embolus-negative, estrogen and progesterone receptor-positive, p53-negative, and Ki67 index less than 14%. Six patients met the requirements and entered the Luminal B Ki67+ group; the patient characteristics in this group were: no lymph node metastases, histological grade I, Her2-negative, vascular cancer embolus-negative, estrogen and progesterone receptor-positive, p53-negative, and Ki67 greater more than or equal to 14%. Six patients met the requirements and entered the Luminal B Her2+ group; the patient characteristics in this group were: lymph node metastases, Her2-positive, vascular cancer embolus-positive, and estrogen receptor-positive. Six met the requirements and entered the Her2 overexpression group; the patient characteristics in this group were: lymph node metastases, histological grade III, Her2-positive, vascular cancer embolus-positive, estrogen and progesterone receptor-negative, p53-positive, and Ki67 greater more than or equal to 14%. Six met the requirements and entered the triple-negative breast cancer (TNBC) group; the patient characteristics in this group were: lymph node metastases, histological grade III, Her2-negative, vascular cancer embolus-positive, estrogen and progesterone receptor-negative, p53-positive, Ki67 greater more than or equal to 14%, and epidermal growth factor receptor (EGFR) or cytokeratin 5/6 (CK5/6)-positive (Table 1). Fluorescence in situ hybridization (FISH) analysis was performed on insulin-like growth factor 1 receptor (IGF1R) and EGFR protein overexpression (IHC+) tumors using the PathVysion HER2 DNA Probe Kit (Vysis; Downers Grove, IL, USA). Her2-positive staining was defined as FISH-positive, and Her2-negative staining was defined as IHC 0 or FISH-negative. We randomly chose 6 patients with benign tumors and normal breast tissues for the control group. All patients gave informed consent and signed the Informed Consent Sheet. This study was approved by the Ethics Committee of Shengjing Hospital.

Tumor samples

The largest section of the tumor, which was parallel

to the chest wall and more than 3 mm thick, was obtained by open surgery. The center and edge of the tumor were determined by eye, and the weight of each specimen was more than 30 mg (Figure 1A). Similar quantities of normal breast tissue were obtained from patients in the control group. All samples were stored at -80°C after quick freezing in liquid nitrogen.

MiRNA array

Since the entry criterion was stringent, it took a long time to collect each group of tumors. Therefore, we first collected samples for miRNA array from the Luminal A and Her2 overexpression groups. For each group of 6 samples, the center and edge fragments of the tumor were mixed with a similar sample from the control group; five such mixed samples (the central part of Luminal A - LA, the edge part of Luminal A - LB, the central part of Her2 overexpression - HA, the edge part of Her2 overexpression - HB, and Normal) were screened using miRNA arrays. The 6th generation miRCURYTM LNA Array (v.16.0) (Exiqon; Vedbaek, Denmari) contains more than 1891 capture probes, covering all human, mouse, and rat miRNAs annotated in miRBase 16.0, as well as all viral miRNAs related to these species. In addition, this array contains capture probes for 66 new miRPlus™ human miRNAs. Total RNA was isolated using TRIzol (Invitrogen; Carlsbad, CA, USA); the miRNeasy Mini Kit (QIAGEN; Spoorstraat, Netherlands) was used to obtain all RNA species, including miRNAs, according to the manufacturer's instructions,. RNA quality and quantity were measured using a nanodrop spectrophotometer (ND-1000, Nanodrop Technologies; Wilmington, DE, USA), and RNA integrity was determined by gel electrophoresis. After RNA isolation from the samples, the miRCURY™ Hy3™/Hy5™ Power labeling kit (Exiqon) was used according to the manufacturer's guidelines for miRNA labeling. One microgram of each sample was 3'-end-labeled with a Hy3TM fluorescent label, using T4 RNA ligase according to the procedure described below. Briefly, RNA in 2.0 μl of water was combined with 1.0 μl CIP buffer and CIP (Exiqon). The mixture was incubated for 30 min at 37°C, and was terminated by incubation for 5 min at 95°C. Then, 3.0 μl of labeling buffer, 1.5 μl of fluorescent label (Hy3TM), 2.0 μl of DMSO, and 2.0 μl of labeling enzyme were added to the mixture. The labeling reaction was incubated for 1 h at 16°C, and terminated by incubation for 15 min at 65°C. The Hy3TM-labeled samples were hybridized on the miRCURYTM LNA Array (v. 16.0) (Exiqon), according to the instructions in the array manual. The 25-μl mixture of Hy3TM-labeled samples and 25 μl hybridization buffer were denatured for 2 min at 95 °C, incubated on ice for 2 min, and then hybridized to the microarray for 16–20 h at 56°C in the 12-Bay Hybridization System (Hybridization System-Nimblegen Systems, Inc.; Madison, WI, USA), which provides active mixing action and constant incubation temperature to improve hybridization uniformity and enhance signals. Following hybridization, the slides were washed several times with wash buffer from the Exiqon kit, and finally, dried by centrifugation for 5 min at 400 rpm. The slides were then scanned using Axon GenePix 4000B microarray scanner (Axon Instruments; Foster City, CA, USA).

Next, samples from Luminal B Ki67+, Luminal B Her2+, and TNBC groups were collected for microarray. For each group of 6 samples, the center and edge fragments of the tumor were mixed with a similar sample from the control group; seven such mixed samples (the central part of Luminal B Ki67+ - LBKC, the edge part of Luminal B Ki67+ - LBKE, the central part of Luminal B Her2+ - LBHC, the edge part of Luminal B Her2+ - LBHE, the central part of TNBC - TNBCC, the edge part of TNBC - TNBCE, and Normal) were screened using miRNA arrays. Here, we performed the microarrays with the 7th generation of miRCURYTM LNA Array (v.18.0) (Exiqon), which contains 3100 capture probes, covering all human, mouse, and rat miRNAs annotated in miRBase 18.0, as well as all viral miRNAs related to these species. The experimental process was basically the same as the aforementioned protocol. These two screening procedures used the same control group.

Statistical analysis

Scanned images were imported into GenePix Pro 6.0 software (Axon) for grid alignment and data extraction. Replicated miRNAs were averaged, and miRNAs with intensities>=50 in all samples were chosen for calculating the normalization factor. Expressed data were normalized using the median normalization. After normalization, differentially expressed miRNAs were identified through Fold Change filtering. Hierarchical clustering was performed using MEV software (v 4.6, TIGR). Differentially expressed miRNAs screening: Contains differentially expressed miRNAs only passed Fold Change filtering (Fold Change>=2.0). All differentially expression miRNAs were comparatively analyzed with Excel (Microsoft Office 2007, Microsoft Corp. Washington, Seattle, USA).

Results

Preliminary identification of differentially expressed miRNAs in breast cancer

We obtained 6 kinds of patterns in the differentially expressed miRNAs for each clinicopathological subtype which included: center/normal≥2; center/normal≤0.5; center/edge≥2; center/edge≤0.5; edge/normal≥2; edge/normal≤0.5 (Figure 1B). Four series of comparative analyses were performed in the 6 kinds of data which included: center/normal≥2 vs center/edge≥2 vs edge/normal≥2; center/normal≥2 vs center/edge≤0.5 vs edge/normal≥2; center/normal≤0.5 vs center/edge≥2 vs edge/normal≤0.5; center/normal≤0.5 vs center/edge≤0.5 vs edge/normal≤0.5. We obtained 4 sequences of miRNA expression for each clinicopathological subtype: center>edge>normal; edge>center>normal; edge<center<normal; center<edge<normal (Figure 2). There were no miRNAs in accordance with LA>LB>Normal, LB>LA>Normal, LB<LA<Normal, HA>HB>Normal, HB>HA>Normal, and HA<HB<Normal. Fourteen series of miRNAs are shown in Table 2, which includes 8 kinds of miRNAs for Luminal A subtype, 84 kinds for Luminal

Table 2. Differential Distribution of miRNAs According to Each Clinicopathological Subtype

	Center>Edge>Normal	Edge>Center>Normal	Edge<Center<Normal	Center<Edge<Normal
Luminal A -8				hsa-miR-140-5p hsa-miR-10b hsa-miR-3189-3p hsa-miR-20b hsa-miR-374a hsa-miR-20a hsa-miR-335 hsa-miR-190
Luminal B Ki67+ -84	hsa-miR-4326 hsa-miR-593-5p ebv-miR-BART11-3p	kshv-miR-K12-7-5p hsa-miR-325 hsa-miR-2114-3p hsa-miR-676-3p hsa-miR-381-5p hsa-miR-506-3p hsa-miR-4320 hsa-miR-504 hsa-miR-346 sv40-miR-S1-3p hsa-miR-767-3p hsa-miR-1288 hsa-miR-204-5p hsa-miR-648 hsa-miR-18b-3p hsa-miR-520a-3p hsa-miR-616-5p hsa-miR-618 hsa-miR-615-5p hsa-miR-4269 hsa-miR-1225-3p hsa-miR-1909-5p hsa-miR-431-5p hcmv-miR-US33-5p hsa-miR-1267	hsa-let-7f-5p; hsa-miR-93-5p hsa-miR-19a-3p; hsa-miR-32-5p hsa-miR-143-3p; hsa-miR-16-5p hsa-miR-3653; hsa-miR-146a-5p hsa-miR-15a-5p; hsa-let-7b-5p hsa-miR-15b-5p; hsa-miR-126-3p hsa-miR-29c-3p; hsa-miR-26b-5p hsa-miR-30a-5p; hsa-miR-19b-3p hsa-miR-148a-3p; hsa-miR-30e-5p hsa-let-7a-5p; hsa-miR-30b-5p hsa-miR-106b-5p;hsa-miR-3607-3p hsa-miR-29b-3p; hsa-miR-142-5p hsa-miR-100-5p; hsa-miR-140-3p hsa-miR-96-5p; hsa-miR-181a-5p hsa-miR-148b-3p; hsa-miR-195-5p hsa-miR-23a-3p; hsa-miR-424-5p hsa-miR-335-5p; hsa-miR-199a-3p/hsa-miR-199b-3p hsa-miR-24-3p; hsa-miR-30a-3p hsa-miR-374a-5p; hsa-miR-665 hsa-miR-26a-5p; hsa-miR-30c-5p hsa-miR-342-3p; hsa-miR-497-5p hsa-let-7i-5p; hsa-miR-98-5p hsa-miR-374b-5p; hsa-miR-542-3p	hsa-miR-126-5p hsa-miR-30c-2-3p hsa-miR-4289 hsa-miR-127-3p hsa-miR-135a-5p hsa-miR-3621 hsa-miR-30c-1-3p hsa-miR-99a-3p hsv2-miR-H6-5p hsa-miR-3180/ hsa-miR-3180-3p
Luminal B Her2+ -52	hsa-miR-148b-5p hsa-miR-3681-5p hsa-miR-1298 hsa-miR-190b hsa-miR-297 hsa-miR-155-5p hsa-miR-183-5p hsa-miR-3183 hsa-miR-105-3p hsa-miR-149-5p	hsa-miR-2113 hsa-miR-1207-3p hsa-miR-3614-3p mcv-miR-M1-3p hsa-miR-34c-3p hsa-miR-219-1-3p	hsa-miR-135a-5p; hcmv-miR-US33-3p hsa-miR-3180/hsa-miR-3180-3p hsa-miR-3609; hsa-miR-497-5p hsa-miR-483-5p; hsa-miR-26b-5p hsa-miR-136-5p; hsa-miR-32-5p hsa-miR-140-5p; hsa-miR-130a-3p hsa-miR-10b-5p; hsa-miR-30a-5p hsa-miR-30c-1-3p hsa-miR-335-5p; hsa-miR-126-3p hsa-miR-100-5p; hsa-miR-377-3p hsa-miR-337-5p; hsa-miR-376c-3p hsa-miR-125b-5p	hsa-miR-1915-3p hsa-miR-451a hsa-miR-492 hsa-miR-185-5p hsa-miR-374b-5p hsa-miR-4306 hsa-miR-1224-3p hsa-miR-10a-5p hsa-miR-30e-5p hsa-miR-197-3p hsa-miR-3653 hsa-miR-151a-5p hsa-miR-30b-5p hsa-miR-143-3p hsa-miR-205-5p
Her2 OE -13			hsa-miR-20a; hsa-miR-335 hsa-miR-30b; hsa-miR-374a hsa-miR-126*; hsa-miR-30e hsa-miR-27a; hsa-miR-374c hsa-miR-20b; hsa-miR-10b hsa-miR-143; hsa-miR-126 hsa-miR-3607-3p	
TNBC (Basal Like) -50	hsa-miR-942 hsa-miR-412 hsa-miR-122-3p hsa-miR-4297 hsa-miR-632	hsa-miR-3180-5p hsa-miR-3614-3p hsa-miR-518e-3p hsa-miR-521 hsa-miR-3913-5p hsa-miR-1225-5p hsa-miR-190b	hsa-miR-142-3p; hsa-miR-199a-5p hsa-miR-15a-5p; hsa-miR-20a-5p hsa-miR-664a-5p hsa-miR-3607-5p hsa-miR-126-3p; hsa-miR-93-5p hsa-let-7a-5p; hsa-miR-29c-3p hsa-miR-21-5p; hsa-miR-148a-3p hsa-miR-33a-5p; hsa-miR-9-5p hsa-miR-142-5p; hsa-miR-195-5p hsa-miR-152; hsa-miR-140-3p hsa-let-7g-5p; hsa-miR-196a-5p hsa-miR-145-5p; hsa-miR-26a-5p hsa-miR-22-3p; hsa-miR-374a-5p	hsa-miR-30c-1-3p hsa-miR-1469 hsa-miR-204-3p hsa-miR-744-5p hsa-miR-711 hsa-miR-542-3p hsa-miR-451a hsa-miR-483-5p hsa-miR-1908 hsa-miR-24-3p hsa-miR-30e-5p hsa-miR-374c-5p hsa-miR-3196 hsa-miR-144-3p

Description: According to the analyses shown in Figure 2, we find that 8 kinds of mRNAs were differentially distributed in Luminal A tumors, 84 kinds in Luminal B Ki67+ tumors, 52 kinds in Luminal B Her+ tumors, 13 kinds in Her2 overexpression tumors, and 50 kinds in TNBC tumors

Table 3. Differential Distribution of miRNAs in Different Subtypes (17 kinds of miRNAs) & same miRNA Distribution between Each Subtype (20 kinds of miRNAs)

Center>Edge>Normal	Edge>Center>Normal	Edge<Center<Normal	Center<Edge<Normal	Number
Luminal A			hsa-miR-140-5p	1
Luminal B Her2+		hsa-miR-140-5p		
Luminal A			hsa-miR-374a	4
			hsa-miR-335	
			hsa-miR-20b	
			hsa-miR-20a	
			hsa-miR-10b	
Her2 OE			hsa-miR-374a	
		hsa-miR-335		
		hsa-miR-20b		
		hsa-miR-20a		
		hsa-miR-10b		
Luminal B Ki67+		hsa-miR-143-3p	hsa-miR-135a-5p	6
		hsa-miR-3653	hsa-miR-3180/hsa-miR-3180-3p	
		hsa-miR-30b-5p		
		hsa-miR-374b-5p		
Luminal B Her2+		hsa-miR-135a-5p	hsa-miR-143-3p	
		hsa-miR-3180/	hsa-miR-3653	
		hsa-miR-3180-3p	hsa-miR-30b-5p	
		hsa-miR-374b-5p		
Luminal B Ki67+		hsa-miR-24-3p		2
		hsa-miR-542-3p		
TNBC (Basal Like)			hsa-miR-24-3p	
			hsa-miR-542-3p	
Luminal B Her2+	hsa-miR-190b	hsa-miR-483-5p		2
TNBC (Basal Like)		hsa-miR-190b	hsa-miR-483-5p	
Luminal B Ki67+		hsa-miR-30e-5p	hsa-miR-30c-1-3p	2
Luminal B Her2+		hsa-miR-30c-1-3p	hsa-miR-30e-5p	
TNBC (Basal Like)			hsa-miR-30e-5p	
			hsa-miR-30c-1-3p	
Luminal B Ki67+		hsa-miR-32-5p		6
vs		hsa-miR-26b-5p		
Luminal B Her2+		hsa-miR-30a-5p		
		hsa-miR-100-5p		
		hsa-miR-335-5p		
		hsa-miR-497-5p		
Luminal B Ki67+		hsa-miR-3607-3p		1
vs				
Her2 OE				
Luminal B Ki67+		hsa-miR-93-5p		10
vs		hsa-miR-15a-5p		
TNBC (Basal Like)		hsa-miR-29c-3p		
		hsa-miR-148a-3p		
		hsa-let-7a-5p		
		hsa-miR-142-5p		
		hsa-miR-140-3p		
		hsa-miR-195-5p		
		hsa-miR-374a-5p		
		hsa-miR-26a-5p		
Luminal B Her2+	hsa-miR-3614-3p		hsa-miR-451a	2
vs				
TNBC (Basal Like)				
Luminal B Ki67+		hsa-miR-126-3p		1
vs				
Luminal B Her2+				
vs				
TNBC (Basal Like)				

Description: According to the comparison of miRNAs shown in Table 2, we find 1 kind of microRNA differentially distributed between Luminal A and Luminal B Her2+ tumors, 5 kinds between Luminal A and Her2 overexpression tumors, 6 kinds between Luminal B Ki67+ and Luminal B Her2+ tumors, 2 kinds between Luminal B Ki67+ and TNBC tumors, 2 kinds between Luminal B Her2+ and TNBC tumors, and 2 kinds between Luminal B Ki67+, Luminal B Her2+, and TNBC tumors. We also find that 6 of the same types of microRNAs were distributed in both Luminal B Ki67+ and Luminal B Her2+ tumors, 1 kind in both Luminal B Ki67+ and Her2 OE tumors, 10 kinds in both Luminal B Ki67+ and TNBC tumors, 2 kinds in both Luminal B Her2+ and TNBC tumors, and one kind in Luminal B Ki67+, Luminal B Her2+, and TNBC tumors

B Ki67+ subtype, 52 kinds for Luminal B Her2+ subtype, 13 kinds for Her2 overexpression subtype, and 50 kinds for TNBC subtype (Table 2).

Differentially expressed microRNAs

All miRNAs were comparatively analyzed by Excel, and repeat miRNAs were obtained between all clinicopathological subtypes. Seventeen kinds of miRNAs were heterogeneously distributed in the tumor from different clinicopathological subtypes that included: 1 kind of miRNA in Luminal A and Luminal B Her2+ subtypes, 4 kinds between Luminal A and Her2 overexpression subtypes, 6 kinds between Luminal B Ki67+ and Luminal B Her2+ subtypes, 2 kinds between Luminal B Ki67+ and TNBC subtypes, 2 kinds between Luminal B Her2+ and TNBC subtypes, and 2 kinds between luminal B

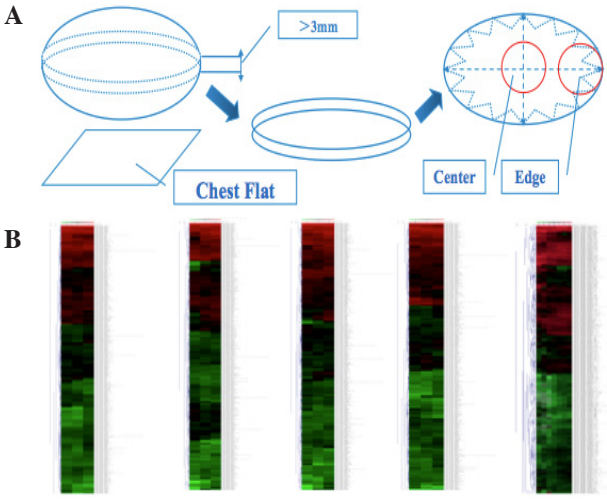

Figure 1. Tumor & MicroRNA-Array. (A): Diagram of Tumor Partition; (B): Clustering of Normalized miRNAs. Description: The aim was to lay the chest flat so that the tumor's edge was located between the tumor and the normal breast tissue. Microarrays were first performed in tumors of the Luminal A and Her2 overexpression subtypes, which are marked with L and H, followed by microarrays in the Luminal B Ki67+, Luminal B Her+, and TNBC subtypes

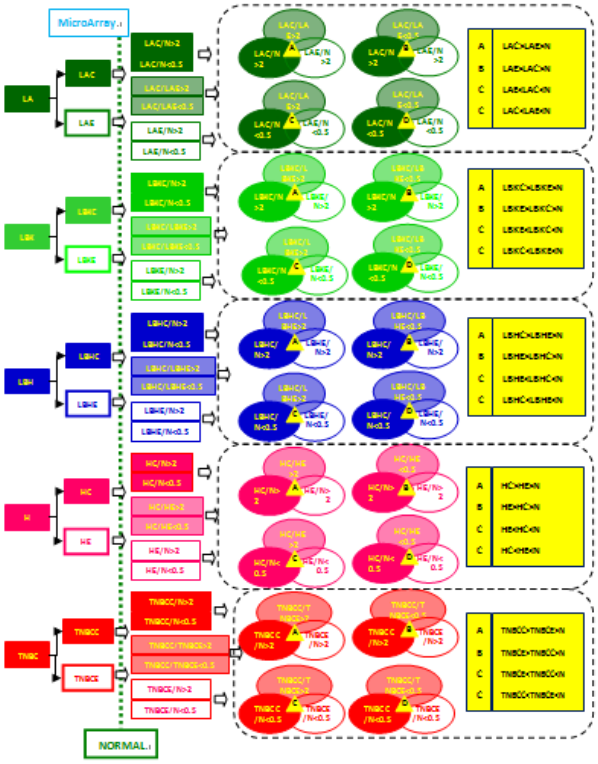

Figure 2. The Workflow of Microarray and Data Analysis. Description: As the workflow shows, we obtained 4 kinds of expression patterns, which included A (center>edge>normal), B (edge>center>normal), C (edge<center<normal), and D (center<edge<normal)

Ki67+, Luminal B Her2+, and TNBC subtypes (Table 3). Twenty kinds of miRNAs were homogenously distributed in tumors from different clinicopathological subtypes that included: 6 kinds of miRNAs between Luminal B Ki67+ and Luminal B Her2+ subtypes, 1 kind between Luminal B Ki67+ and Her2 overexpression subtypes, 10 kinds between Luminal B Ki67+ and TNBC subtypes, 2

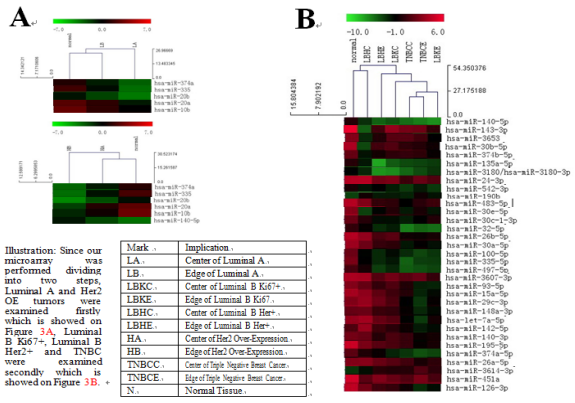

Figure 3. The miRNAs Significant Distributed in Tumor

kinds between Luminal B Her2+ and TNBC subtypes, and 1 kind between Luminal B Ki67+, Luminal B Her2+, and TNBC subtypes (Table 3). A total of 37 miRNAs were significantly distributed in tumors between all clinicopathological subtypes (Figure 3).

Discussion

Oncologists engage in discussion on cancer heterogeneity between individuals with more enthusiasm than they do when discussing the heterogeneity of the cancer itself, even though it has long been known that solid cancer is a heterogenous tissue with differential oxygen pressure, histological grade, and mRNA expression (Wilson et al., 1992; Aihara et al., 1994; Kitadai et al., 1995). In addition, it has become gradually accepted that applying competition colonization tradeoff models to tumor growth and invasion dynamics can be useful for exploring the hypothesis that varying selection forces will result in predictable phenotypic differences in cells at the tumor invasive front compared to those in the core (Orlando et al., 2013).

As shown in Table 1, the diameter of a breast tumor must be more than or equal to 2 cm for the center and edge to be easily distinguished, according to Figure 1A. A recent study suggested that some key miRNAs may play signaling or regulatory roles in cancer progression (Hughes, 2009). On the other hand, the 12th St Gallen International Breast Cancer Conference (2011) Expert Panel adopted a new approach for classifying patients for therapeutic purposes based on the recognition of intrinsic biological subtypes within the breast cancer spectrum, which can be classified by immunohistochemical staining (Goldhirsch et al., 2011). Therefore, we performed miRNA Arrays on the center and edges of tumors from different clinicopathological subtypes. Eleven types of expression profiles were obtained (Figure 1A), which included 5 center samples and 5 edge samples from 5 subtypes and 1 normal tissue (Figure 1B). Because all neoplastic parenchyma cells share at least one primary chromosomal abnormality, with subsequent clonal evolution along the lines of Darwinian selection occurring among various subclones carrying secondary aberrations (Teixeira et al, 2011). We analyzed data under the hypothesis of tumorigenesis. First, abnormal orders of miRNA expression

were removed that included edge<normal<center and center<normal<edge. Second, we obtained 4 orders of miRNA expression in each clinicopathological subtype, which included center>edge>normal, edge>center>normal, edge<center<normal, and center<edge<normal (Figure 2). Therefore, 8 kinds of miRNAs were differentially distributed in Luminal A, 84 kinds in Luminal B Ki67+, 52 kinds in Luminal B Her2+, 13 kinds in Her2 overexpression, and 50 kinds in TNBC subtypes (Table 2). Furthermore, by comparative analyses, we found that 17 miRNAs were heterogeneously distributed in different clinicopathological subtypes, and 20 miRNAs were homogeneously distributed (Tables 3, Figure 3). With imaging times of less than 3 minutes by electron paramagnetic resonance imaging, it was possible to monitor the dynamics of oxygen changes in the tumors, and to chronically distinguish hypoxic regions from acutely hypoxic regions (Krishna et al., 2012). We speculated that these differentially expressed miRNAs were probably related to degree of hypoxia, or even with angiogenesis. Therefore, we performed predictive analyses on miR-374a, -335, -20b, -20a, and -10b using bioinformatic tools (www.microrna.org), and found that miR-20a and miR-20b likely regulate target proteins, including vascular endothelial growth factor-A (VEGF-A) and hypoxia-inducible factor-1 (HIF-1), at the translational level. This regulatory mechanism was proven preliminarily with clinical experiments and subsequently published by Li et al (2012).

Tumorigenesis and progression can be seen as evolutionary processes, in which the transformation of a normal cell into a tumor cell involves a number of limiting genetic and epigenetic events that occur in a series of discrete stages (Stransky et al, 2012). Both functional and observational data implicate alterations in histone modifications, DNA promoter methylation, and non-coding RNA expression in carcinogenesis (Choudhry et al, 2011). On the other hand, due to the wide range of biological functions of miRNAs, analyzing changes in overall miRNA expression levels within human tumors has helped identify miRNA signatures associated with diagnosis, staging, progression, prognosis, and response to treatment (Cortés-Sempere et al, 2011). Thus, the miRNA Array screening of tumors from their centers and edges might provide a new method for studying cancer heterogeneity.

Acknowledgements

This research was supported by the Science and Technology Foundation of Liaoning Province, China (No. 2012225016). The author(s) declare that they have no competing interests.

References

Aihara M, Wheeler TM, Ohori M, et al (1994) Heterogeneity of prostate cancer in radical prostatectomy specimens. *Urology*, **43**, 60-6

Balsat C, Blacher S, Signolle N, et al (2011). Whole slide quantification of stromal lymphatic vessel distribution and peritumoral lymphatic vessel density in early invasive cervical cancer: a method description. *ISRN Obstet Gynecol*, **25**, 1-7.

Caporali A, Emanueli C (2011). MicroRNA regulation in angiogenesis. *Vascul Pharmacol*, **55**, 79-86.

Cheng C, Fu X, Alves P, et al (2009). mRNA expression profiles show differential regulatory effects of microRNAs between estrogen receptor-positive and estrogen receptor-negative breast cancer. *Genome Biol*, **10**, R90.

Choudhry H, Catto JW (2011). Epigenetic regulation of microRNA expression in cancer. *Methods Mol Biol*, **676**, 165-84.

Cortés-Sempere M, Ibáñez de Cáceres I (2011). microRNAs as novel epigenetic biomarkers for human cancer. *Clin Transl Oncol*, **13**, 357-62

Goldhirsch A, Wood WC, Coates AS, et al (2011). Strategies for subtypes--dealing with the diversity of breast cancer: highlights of the St. Gallen International Expert Consensus on the Primary Therapy of Early Breast Cancer 2011. *Ann Oncol*, **22**, 1736-47.

Hughes DP (2009). How the NOTCH pathway contributes to the ability of osteosarcoma cells to metastasize. *Cancer Treat Res*, **152**, 479-96

Iorio MV, Ferracin M, Liu CG, et al (2005). MicroRNA gene expression deregulation in human breast cancer. *Cancer Res*, **65**, 7065-70

Juan HF, Huang HC (2007). Bioinformatics: microarray data clustering and functional classification. *Methods Mol Biol*, **382**, 405-16.

Kitadai Y, Ellis LM, Takahashi Y, et al (1995). Multiparametric in situ messenger RNA hybridization analysis to detect metastasis-related genes in surgical specimens of human colon carcinomas. *Clin Cancer Res*, **1**, 1095-102.

Kreiner T, Buck KT (2005). Moving toward whole-genome analysis: a technology perspective. *Am J Health Syst Pharm*, **62**, 296-305.

Krishna MC, Matsumoto S, Yasui H, et al (2012). Electron paramagnetic resonance imaging of tumor pO_2. *Radiat Res*, **177**, 376-86

Li JY, Zhang Y, Zhang WH, et al (2012). Differential distribution of miR-20a and miR-20b may underly metastatic heterogeneity of breast cancers. *Asian Pac J Cancer Prev*, **13**, 1901-6.

Orlando PA, Gatenby RA, Brown JS (2013). Tumor evolution in space: the effects of competition colonization tradeoffs on tumor invasion dynamics. *Front Oncol*, **3**, 45.

Pritchard CC, Cheng HH, Tewari M (2012). MicroRNA profiling: approaches and considerations. *Nat Rev Genet*, **13**, 358-69.

Stransky B, de Souza SJ (2012). Modeling tumor evolutionary dynamics. *Front Physiol*, **3**, 480.

Teixeira MR, Heim S (2011). Cytogenetic analysis of tumor clonality. *Adv Cancer Res*, **112**, 127-49

Wilson DF, Cerniglia GJ (1992). Localization of tumors and evaluation of their state of oxygenation by phosphorescence imaging. *Cancer Res*, **52**, 3988-93.